



Variability of the surface boundary layer of reef-building coral species

Catarina P. P. Martins¹ · Marlene Wall² · Patrick Schubert¹ ·
Thomas Wilke¹ · Maren Ziegler¹

Received: 22 November 2023 / Accepted: 30 June 2024 / Published online: 15 July 2024
© The Author(s) 2024

Abstract The coral-seawater interface is an important, highly dynamic microenvironment for reef-building corals. Also known as the concentration boundary layer (CBL), it is a thin layer of seawater bordering the coral surface that dictates the biochemical exchange between the coral colony and bulk seawater. The CBL is thus a key feature that modulates coral metabolism. However, CBL variation among small-polyped coral species remains largely unknown. Therefore, we recorded over 100 profiles of dissolved O₂ concentration using microsensors to characterize CBL traits (thickness, surface O₂ concentration, and flux) of three small-polyped branching coral species, *Acropora cytherea*, *Pocillopora verrucosa*, and *Porites cylindrica*. Measurements were conducted during light and darkness combined with low or moderate water flow (2 and 6 cm s⁻¹). We found that CBL traits differed among species. CBL thickness was lowest in *A. cytherea*, while *P. verrucosa* showed the largest depletion of surface O₂ in dark and highest dark flux. In addition, we found that O₂ concentration gradients in the CBL occurred with three main profile shapes: diffusive, S-shaped, and complex. While diffusive profiles were the most common profile type, S-shaped and complex profiles were more frequent in *P. verrucosa* and *P. cylindrica*, respectively, and prevailed under low flow. Furthermore, profile types differed

in CBL thickness and flux. Finally, low flow thickened CBLs, enhanced changes in surface O₂ concentration, and reduced flux, compared to moderate flow. Overall, our findings reveal CBL variability among small-polyped branching corals and help understand CBL dynamics in response to changes in light and water flow conditions.

Keywords Reef-building corals · Boundary layer · Water flow · Oxygen gradients

Introduction

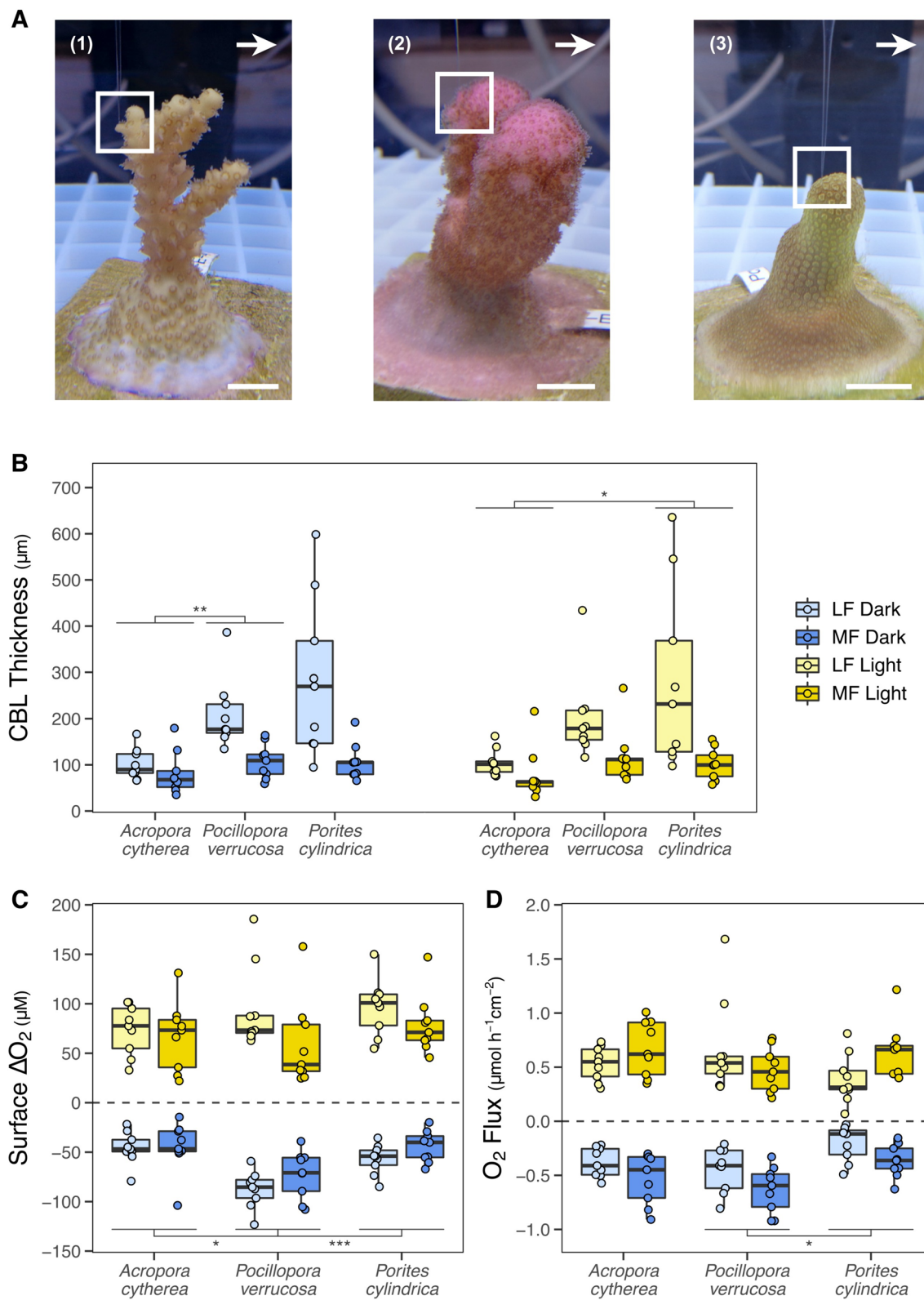
Reef-building corals largely rely on gas exchange with the surrounding seawater to support key physiological processes such as photosynthesis and respiration. This biochemical exchange occurs in the coral boundary layer—a thin layer of seawater bordering the coral surface where concentration gradients of dissolved compounds (e.g., gases and nutrients) between the coral surface and the bulk seawater are formed (Lesser et al. 1994; Thomas and Atkinson 1997). The thickness and structure of the coral boundary layer, which dictate the coral biochemical exchange with seawater (Shashar et al. 1996), are dependent on flow conditions around the colony, coral surface microtopography, and polyp behavior (Shashar et al. 1993). Furthermore, metabolic activity also influences the CBL and may drive changes in CBL traits by altering the build-up of solutes at the coral surface (Hughes et al. 2020). While O₂ concentration gradients are often linear along a so-called diffusive boundary layer (DBL; Jørgensen and Revsbech 1985), they may also have a complex structure due to the presence of surface vortices created by epidermal cilia, particularly under no or slow water flow (Shapiro et al. 2014; Pacherres et al. 2020). Thus, this layer is also referred to as the concentration boundary layer (CBL; Nishihara and

Supplementary Information The online version contains supplementary material available at <https://doi.org/10.1007/s00338-024-02531-7>.

✉ Catarina P. P. Martins
catarina.padilha-pires-martins@bio.uni-giessen.de

¹ Department of Animal Ecology & Systematics, Justus Liebig University Giessen, 35392 Giessen, Germany

² GEOMAR Helmholtz Centre for Ocean Research Kiel, 24148 Kiel, Germany



Ackerman 2007; Noisette et al. 2022), which is the term we use throughout the text.

Variation in CBL traits among coral species leads to differences in colony physiology (Patterson et al. 1991) and has been proposed to underlie differential susceptibility

Fig. 1 Traits of the O₂ concentration boundary layer (CBL) of small-polyped reef-building corals. **A** Photographs of the investigated species during microsensor measurements: (1) *Acropora cytherea*, (2) *Pocillopora verrucosa*, and (3) *Porites cylindrica*. Rectangles mark representative locations of microsensor measurements across coral fragments, and arrows indicate the direction of water flow. Scale bar=1 cm approx. **B** CBL thickness, **C** O₂ concentration change at the coral surface relative to bulk seawater (surface ΔO_2), and **D** O₂ flux, characterized under conditions of light, darkness, low flow (LF, 2 cm s⁻¹), and moderate flow (MF, 6 cm s⁻¹). Boxes represent the first and third quartiles with lines as medians and whiskers as the minimum and maximum values or up to the 1.5 × interquartile range (IQR), whichever is reached first; $n=9$ per species, light, and flow. Stars indicate significant differences between species within light conditions ($p<0.001^{***}$, $p<0.01^{**}$, $p<0.05^*$, from post hoc of LMM-ANOVA)

to climate change effects (Putnam et al. 2017), including coral bleaching (Jimenez et al. 2008). Differences in CBL thickness between large- and small-polyped coral species are well-known, with thicker boundary layers in large-polyped massive species compared to small-polyped species due to the presence of topographical features such as protruding septae (Shashar et al. 1993; Jimenez et al. 2011). Small-polyped species have less differentiating surface features than large-polyped species and would thus be expected to be similar in CBL traits. However, recent studies have shown that coral species, including small-polyped corals, modulate their CBL by creating ciliary vortical flows at the coral surface (Shapiro et al. 2014; Pacherres et al. 2020). This ability to modify the CBL could differ among species, leading to interspecific variability in CBL traits, and thus explain the diversity of physiological rates and susceptibility to climate change effects among small-polyped species. However, variation in CBL traits among small-polyped species remains largely unknown. Furthermore, knowledge of the structure of O₂ concentration gradients within the coral boundary layer and their variability in structure also remains limited.

The aim of this study was to investigate the variability of the CBL of three major reef-building coral species, the small-polyped species *Acropora cytherea*, *Pocillopora verrucosa*, and *Porites cylindrica*. Specifically, we tested (i) whether CBL traits (thickness, surface O₂ concentration, and flux) differed between the three coral species. In addition, we characterized the structure of O₂ concentration gradients within the CBL and assessed (ii) profile structure among species and in response to low and moderate flow (2 and 6 cm s⁻¹) during light and darkness. Finally, we categorized the structure of profiles into three types and investigated (iii) differences in CBL traits among profile types and their response to light and flow. This study will therefore help understand boundary layer variability among reef-building corals and the dynamics of the coral-seawater interface.

Materials and methods

Experimental setup

The O₂ concentration gradient in the coral boundary layer was measured in the small-polyped branching corals *A. cytherea*, *P. verrucosa*, and *P. cylindrica*. Coral colonies (Table S1) were maintained at the ‘Ocean2100’ long-term coral experimental facility at Justus Liebig University Gießen, Germany. Long-term rearing conditions were 11:13 h light:dark photoperiod, with a light intensity of 230 $\mu\text{mol photons m}^{-2} \text{s}^{-1}$, and a temperature of 26.0 ± 0.5 °C for at least six months before the experiment (Martins et al. 2024b). Three colonies per species were cut into three fragments using a small angle grinder (Dremel Multitool 3000-15, The Netherlands) and attached to tiles with two-component glue (CoraFix SuperFast, Grotech, Germany). Measurements were performed six months after fragmentation on fully recovered and healthy fragments.

Profiles of dissolved O₂ concentration were measured using Clark-type O₂ microelectrodes (tip diameter 20–30 μm ; OX-25, Unisense, Denmark) connected to a microsensor multimeter (Unisense, Denmark), whose signals were read on a PC using a 2-channel A/D converter (ADC-216, Unisense, Denmark). Oxygen microsensors were calibrated daily with air-saturated seawater and anoxic seawater prepared using yeast, following manufacturer’s instructions. Profiles were measured on the top upstream face of coral fragments (Fig. 1A), above the coenosarc (connecting tissue between polyps), and on a spot where the tentacles of nearby polyps showed little to no movement. Profiles were performed by carefully placing the tip of the sensor on the coral surface and moving it up in steps of 5–60 μm within the gradient and of 50–200 μm in bulk seawater, using a motorized microprofiling system (Unisense, Denmark). The microsensor was programmed to automatically return to its starting position (i.e., the coral surface) after completing each profile measurement. All measurements were performed on coral fragments with open polyps and extended tentacles. The measuring spot was constantly monitored during all profiles using a stereo microscope (Stemi 508, Carl Zeiss AG, Germany) to verify tentacle extension and avoid artefacts due to tissue movement or polyp interaction. Sensor positioning and data acquisition were performed using the software SensorTrace Profiling (Unisense, Denmark). At each step, values were recorded for 30–60 s with a waiting period of 3 s after moving the sensor. Profiles were conducted in a flume (length 118 cm, width 18 cm, water depth 19 cm) with unidirectional recirculating flow, created by a circulating pump (ES-28, Aqualight, Germany). Flow straighteners were placed up- and downstream of the measurement section (upstream: PVC grid with length of 10.5 cm and 1.3×1.3 cm openings, attached to a layer of nylon net

with 500 μm pore size; downstream: PVC grid with length of 2.5 cm and 1.3×1.3 cm openings).

Microscale oxygen profiles

A total of 108 profiles were recorded. For each coral fragment, profiles were measured in a total of four conditions: light and darkness combined with low (2 cm s^{-1}) and moderate (6 cm s^{-1}) flow conditions ($n=6$ profiles per genotype per species per light condition, $n=6$ profiles per genotype per species per flow condition). To characterize flow conditions around the coral fragments under the two flow velocities, the dimensionless Reynolds number (Re) was calculated as $Re = uW/\nu$ from the flow velocity (u), the coral height (W) (Lesser et al. 1994), and the kinematic viscosity (ν) of seawater at 26°C and salinity 35 (Ramsing and Gundersen 2023). Coral height was estimated from photographs using ImageJ (v2.1.0/1.53c), and coral volume was estimated using 3D scanning (see Supplementary Text for methodological details). Flow conditions around coral fragments were overall similar (Table 1) and corresponded to Re values of 646 and 1,937 for the low and moderate flow velocities, respectively, indicating that the coral fragments experienced laminar flow (Patterson et al. 1991) under both velocities. Measurements were performed after coral fragments had been acclimated to light and flow conditions (light, 10 min; darkness, 5 min; flow, 10 min), and it was ensured that steady-state O_2 conditions had been reached before starting each profile. All flow and light conditions were measured, in succession, on the same spot for each coral fragment during daylight hours. Water temperature was maintained at 26°C , salinity at 35, pH_T at 8.02, O_2 concentration at $240 \pm 8 \mu\text{M}$, and light intensity at $200 \mu\text{mol photons m}^{-2} \text{ s}^{-1}$.

Calculation of boundary layer traits

Oxygen concentration profiles were used to calculate total thickness of the CBL, diffusive flux through the CBL, and change of O_2 concentration at the coral surface relative to ambient seawater (surface ΔO_2). The CBL thickness was determined as the distance between the coral surface and the outer limit of the upper diffusive boundary layer (Pacherres et al. 2020), calculated by extrapolating the linear

concentration gradient in the CBL to the ambient seawater concentration of the free-flow region (Jørgensen and Revsbech 1985). Oxygen flux was calculated using Fick's first law of diffusion (Jørgensen and Revsbech 1985; Nishihara and Ackerman 2007) with O_2 diffusion coefficient of $2.29 \times 10^{-5} \text{ cm}^2 \text{ s}^{-1}$ at 26.0°C and salinity of 35 (Ramsing and Gundersen 2023). Our data contained both linear and nonlinear profiles. To calculate CBL thickness and O_2 flux of nonlinear profiles using Fick's first law of diffusion, we followed the protocol developed by Pacherres et al. (2020) and used the upper linear gradient of the profiles—i.e., the linear gradient that preceded bulk seawater concentration. Flow in the upper linear gradient is laminar and calculations using this part of the profile provide a representative estimation of the flux across the coral CBL, without needing to resolve the mechanisms in the more complex, nonlinear parts of the profile (Pacherres et al. 2020). Additional details on our rationale for the chosen approach can be found in Martins et al. (2024b).

Statistical analysis

Oxygen concentration profiles were grouped by common characteristics, and the total number of profiles per profile type was recorded. Differences in CBL thickness, surface ΔO_2 concentration, and O_2 flux between profile types in light and darkness were assessed using linear mixed-effects models (LMMs). All models were constructed with profile type (3 levels: diffusive, S-shaped, and complex), species (3 levels: *A. cytherea*, *P. verrucosa*, and *P. cylindrica*) and flow (2 levels: low and moderate) as fixed factors, and coral fragment identity (ID) as random factor. Linear mixed-effects models were performed using the *R* package *lme4* (Bates et al. 2015). Model validation was done by graphically assessing homogeneity and normality assumptions. To meet model assumptions, we applied a log transformation to light and dark CBL thickness and light O_2 flux, followed by an inspection of the shape of trends. Models were selected based on AIC, BIC and R^2 values. Numerical output and model formulas of LMMs are given in Table S2. We then computed type-II ANOVA tables of the fixed effects of LMMs using Kenward–Roger approximation for the degrees of freedom in the *R* package *car* (Fox and Weisberg

Table 1 Dimensions (mean \pm SD) of the investigated coral fragments of *Acropora cytherea*, *Pocillopora verrucosa*, and *Porites cylindrica* and the calculated dimensionless Reynolds number correspond-

ing to low (Re_{LF}) and moderate (Re_{MF}) water flow velocities (2 and 6 cm s^{-1} , respectively)

Species	Height (cm)	Volume (cm^3)	Shape	Re_{LF}	Re_{MF}
<i>Acropora cytherea</i>	3.3 ± 0.4	3.7 ± 0.8	Branching	718 ± 93	$2,153 \pm 279$
<i>Pocillopora verrucosa</i>	3.0 ± 0.6	7.5 ± 1.8	Branching	661 ± 120	$1,983 \pm 361$
<i>Porites cylindrica</i>	2.6 ± 0.3	4.7 ± 1.2	Columnar	559 ± 62	$1,676 \pm 186$

2019). Post hoc analyses were performed using the *R* package *emmeans* (Lenth 2021) with Tukey adjustment of *p* values. All plots were produced using the *R* package *ggplot2* (Wickham 2016). All statistical analyses were performed in *R* (v.4.1.0; R Core Team 2021) using RStudio (v1.4.1106; RStudio Team 2021).

Results

Traits of boundary layers differ between species

The three investigated coral species differed in the traits of their O₂ boundary layer, pooled over water flow conditions. CBL thickness differed between species in both light (LMM-ANOVA, $F=4.2$, $p<0.05$) and darkness (LMM-ANOVA, $F=6.6$, $p<0.01$) (Fig. 1B). *Acropora cytherea* generally had a thinner CBL (92 ± 45 μm) than *P. verrucosa* in darkness (159 ± 78 μm ; post hoc, $t=-3.5$, $p<0.01$) and *P. cylindrica* in light (192 ± 165 μm ; post hoc, $t=-2.6$, $p<0.05$), which were not significantly different from each other (light/dark, post hoc, $t=-0.2/0.9$, $p>0.05$). In light, surface ΔO_2 concentration (range: 70.5–87.7 μM) and O₂ flux (range: 0.52–0.60 $\mu\text{mol cm}^{-2} \text{h}^{-1}$) were similar between species (Fig. 1C, D; flux/ ΔO_2 , LMM-ANOVA, $F=0.5/1.0$, $p>0.05$). In contrast, surface ΔO_2 concentration and O₂ flux in darkness differed between species (LMM-ANOVA, $F=3.5/9.7$, $p<0.05/0.001$). Dark surface ΔO_2 concentration was highest in *P. verrucosa* (-80.0 ± 22.1 μM), compared to *A. cytherea* (-45.6 ± 20.6 μM ; post hoc, $t=4.1$, $p<0.001$) and *P. cylindrica* (-50.8 ± 16.3 μM ; post hoc, $t=-3.3$, $p<0.01$), which did not significantly differ from each other (post hoc, $t=0.6$, $p>0.05$) (Fig. 1C). *Pocillopora verrucosa* also had a significantly higher dark O₂ flux (-0.54 ± 0.22 $\mu\text{mol cm}^{-2} \text{h}^{-1}$) than *P. cylindrica* (-0.29 ± 0.17 $\mu\text{mol cm}^{-2} \text{h}^{-1}$; post hoc, $t=-2.6$, $p<0.05$), but not *A. cytherea* (-0.46 ± 0.20 $\mu\text{mol cm}^{-2} \text{h}^{-1}$; post hoc, $t=1.1$, $p>0.05$), which were not significantly different from each other (post hoc, $t=-1.6$, $p>0.05$) (Fig. 1D).

Flow conditions generally modulated CBL traits across species. CBL thickness was overall larger under low flow compared to moderate flow (light/dark, LMM-ANOVA, $F=36.1/39.7$, $p<0.001$), with the smallest increase in *A. cytherea* compared to *P. cylindrica*, which presented a wide range of thickness values (Fig. 1B). Surface ΔO_2 concentration was also larger under low flow compared to moderate flow (light/dark, LMM-ANOVA, $F=12.3/7.7$, $p<0.01/0.05$), but with similar changes across species (Fig. 1C). Flow conditions had a significant effect on O₂ flux in darkness only (LMM-ANOVA; light, $F=1.9$, $p>0.05$; dark, $F=10.9$, $p<0.01$), which was increased under moderate flow compared to low flow (Fig. 1D).

The shape of gradients within the coral boundary layer differs with species and water flow

We found that the O₂ concentration gradient in the CBL had different profile shapes, which we categorized into three main groups: diffusive, S-shaped, and complex. Diffusive profiles were characterized by a single linear concentration gradient, typical of a DBL (Fig. 2A); S-shaped profiles by a distanced linear gradient with a steeper slope at the coral surface (Fig. 2B); and complex profiles by multiple DBLs (Fig. 2C).

Overall, the three profile types were not equally frequent. Diffusive profiles were the most common type of profile (60%), while 32% of all measured profiles were S-shaped and only 8% were complex. The occurrence of the types of profiles differed between species (Fig. 2D). Diffusive profiles were more commonly observed in *A. cytherea* (75%) than in *P. verrucosa* (47%) or *P. cylindrica* (58%). S-shaped profiles were as frequent as diffusive profiles in *P. verrucosa* (50%), and more frequent compared to the other species (*A. cytherea*, 25%; *P. cylindrica*, 19%). In *A. cytherea* no complex profile and in *P. verrucosa* only one complex profile was observed, while they were as common as S-shaped profiles in *P. cylindrica* (22%).

The occurrence of profile types differed with light and flow conditions, depending on the species. In *A. cytherea*, diffusive profiles were the predominant profile type in all conditions (Fig. 2E). In this species, the less frequent S-shaped profiles occurred predominantly under moderate flow and in darkness (Fig. 2E). In *P. verrucosa*, although diffusive and S-shaped profiles were overall equally common, diffusive profiles were more common under low flow in darkness, while S-shaped profiles were more common under low flow in the light (Fig. 2F). Under moderate flow, this pattern was reversed. The two complex profiles observed in *P. verrucosa* occurred in light and under moderate flow. In *P. cylindrica*, diffusive profiles were predominant under all conditions, except in darkness and under low flow, where complex profiles were predominant (Fig. 2G). Similar to *A. cytherea*, S-shaped profiles occurred more frequently in darkness. Complex profiles occurred mostly under low flow, with only one profile observed under moderate flow, which occurred in darkness.

Quantitative traits of boundary layers of different shape

Boundary layers with different profile types were characterized by differences in their traits, which were largely determined by water flow (Table S3). Overall, profile types differed significantly in CBL thickness (light/dark, LMM-ANOVA, $F=9.8/8.7$, $p<0.001$), with complex profiles being three times as thick as diffusive (light/dark, post hoc,

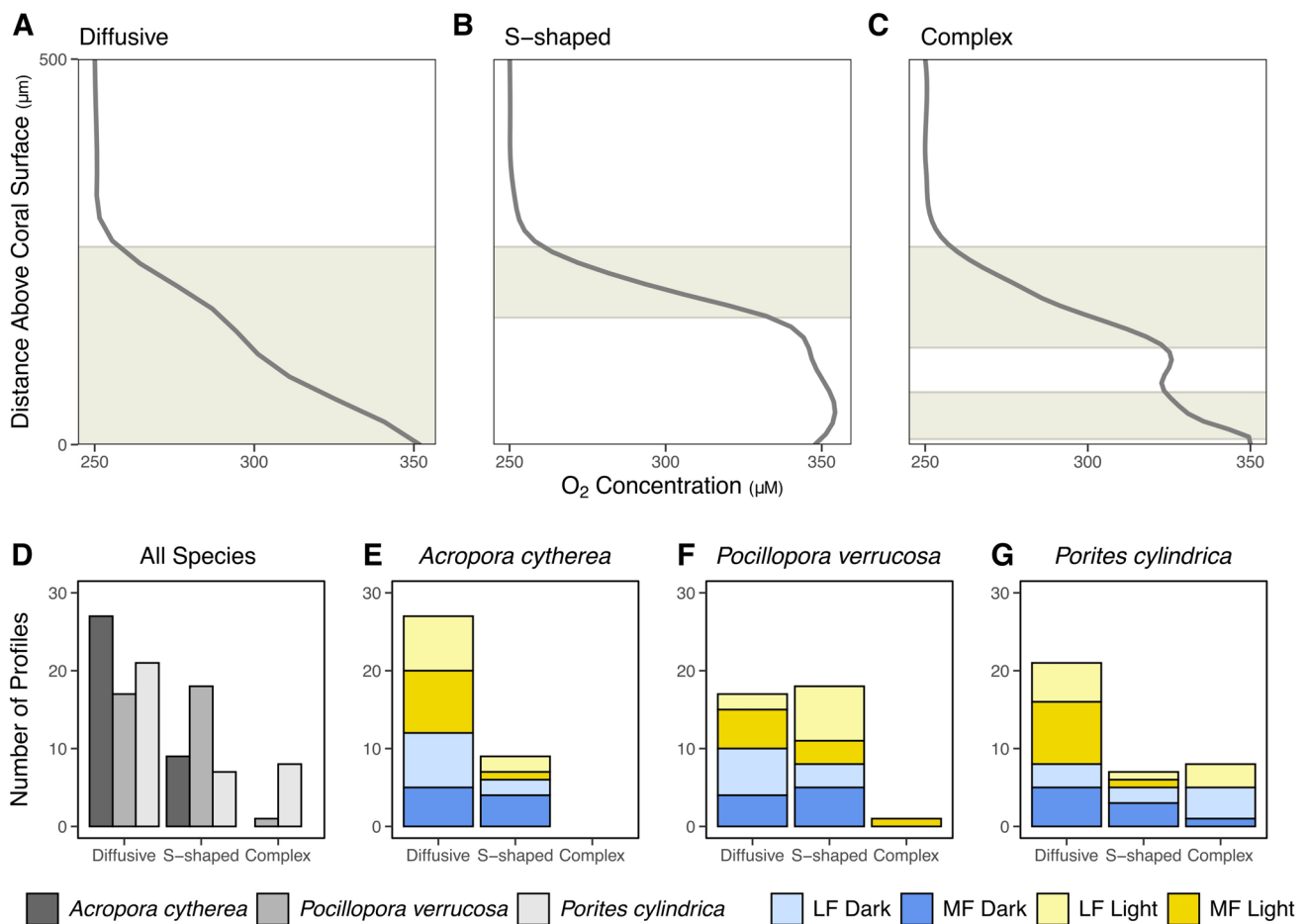


Fig. 2 Variability of O₂ gradients in the concentration boundary layer. Schematic diagrams representing O₂ concentration gradients in the boundary layer of three reef-building coral species with **A** diffusive, **B** S-shaped, and **C** complex structure. Diagrams represent profiles under light conditions, created to facilitate visualization of the three types of profile structure. Visual presentation of all measured profiles, including the individual profiles used to produce the sche-

matic diagrams, is provided in Fig. S1. Shaded areas mark regions where mass transport is dominantly diffusive. **D** Number of profiles of O₂ concentration gradients in the coral boundary layer with diffusive, S-shaped, or complex structure across species and in **E** *Acropora cytherea*, **F** *Pocillopora verrucosa*, and **G** *Porites cylindrica*, in light and darkness, and low flow (LF, 2 cm s⁻¹) or moderate flow (MF, 6 cm s⁻¹)

$t = -4.4 / -4.2$, $p < 0.001$) and S-shaped profiles (light/dark, post hoc, $t = -2.9 / -3.7$, $p < 0.05/0.01$), which were not significantly different from each other (light/dark, post hoc, $t = -1.2 / -0.4$, $p > 0.05$) (Fig. 3A). Under low flow, complex profiles had an average CBL thickness of 437 ± 170 μm, while diffusive and S-shaped profiles had 147 ± 77 and 188 ± 95 μm, respectively. Under moderate flow, CBL thickness was more similar across profile types (diffusive, 93 ± 43 ; S-shaped, 104 ± 50 ; complex, 164 ± 40 μm).

Surface ΔO₂ concentration was overall similar between profile types (light/dark, LMM-ANOVA, $F = 2.7/0.7$, $p > 0.05$; Fig. 3B). In light, O₂ at the coral surface was overall 88.4 ± 33.2 and 68.2 ± 35.9 μM above seawater O₂ concentration under low and moderate flow, respectively. In darkness, it was 63.5 ± 24.1 and 54.1 ± 25.0 μM below

seawater concentration under low and moderate flow, respectively.

Compared to thickness, flux displayed the inverted pattern of profile types (light/dark, LMM-ANOVA, $F = 4.0/10.9$, $p < 0.05/0.001$), with increased values under moderate flow compared to low flow in all profile types (Table S3). Light O₂ flux was overall highest in S-shaped profiles (0.64 ± 0.35 μmol cm⁻² h⁻¹) and significantly higher than complex profiles (0.35 ± 0.28 μmol cm⁻² h⁻¹; post hoc, $t = 2.8$, $p < 0.05$), but not diffusive profiles (0.56 ± 0.24 μmol cm⁻² h⁻¹; post hoc, $t = -1.4$, $p > 0.05$), which were not significantly different from each other (post hoc, $t = 2.2$, $p > 0.05$) (Fig. 3C). In darkness, S-shaped profiles had a significantly higher O₂ flux than both diffusive (post hoc, $t = 3.6$, $p < 0.01$) and complex profiles (post hoc,

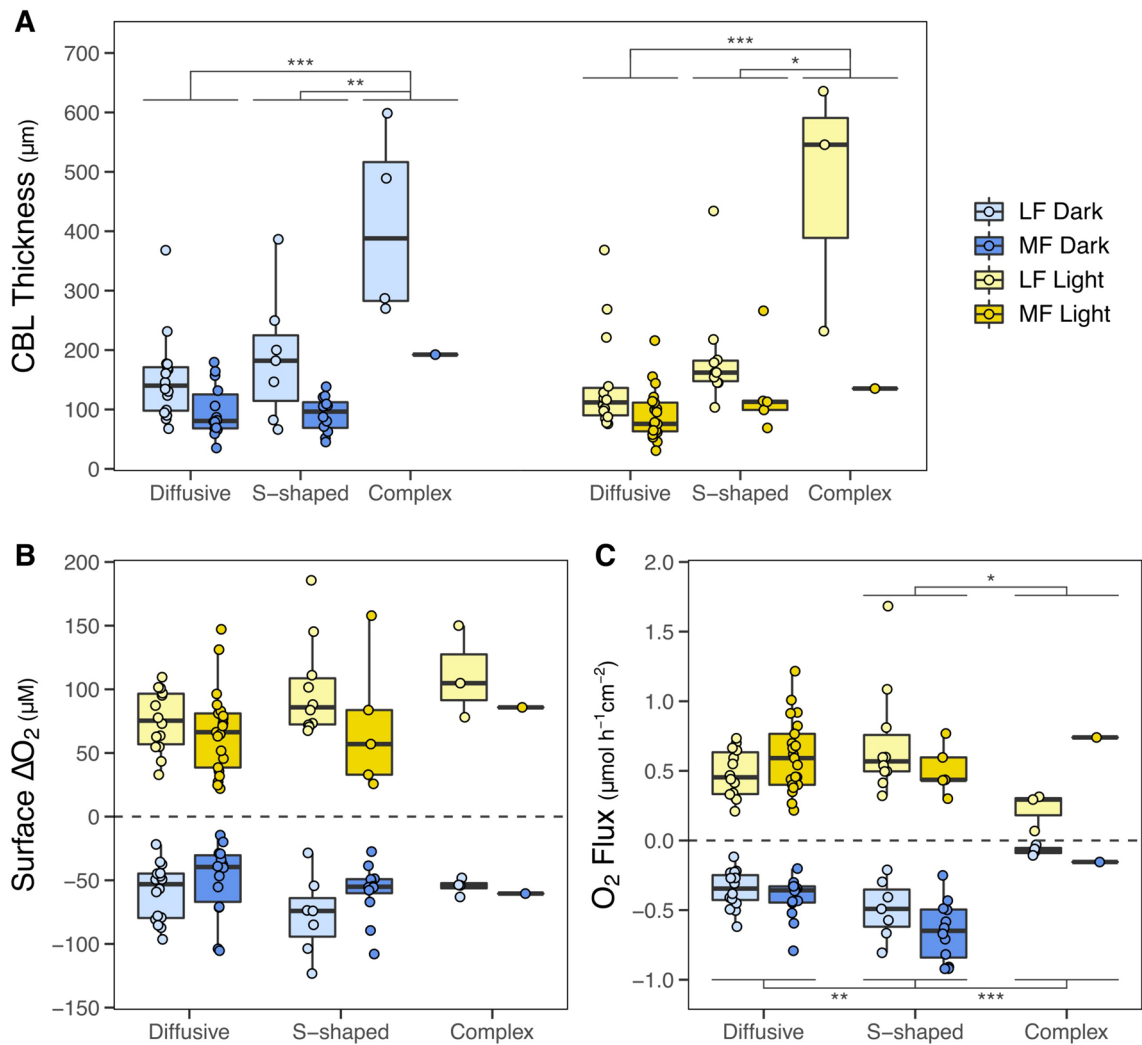


Fig. 3 Traits of profile types (diffusive, S-shaped, and complex) of the concentration boundary layer (CBL) under light and darkness and two levels of water flow. **A** CBL thickness, **B** O_2 concentration change at the coral surface relative to bulk seawater (surface ΔO_2), and **C** O_2 flux, measured in *Acropora cytherea*, *Pocillopora verrucosa*, and *Porites cylindrica*, under conditions of light, darkness, low flow (LF, 2 cm s^{-1}), and moderate flow (MF, 6 cm s^{-1}). Boxes repre-

sented the first and third quartiles with lines as medians and whiskers as the minimum and maximum values or up to the $1.5 \times$ interquartile range (IQR), whichever is reached first; see Table S3 for n . Stars indicate significant differences between profile types pooled over flow conditions in light and darkness ($p < 0.001$ ***, $p < 0.01$ ** , $p < 0.05$ * , from post hoc of LMM-ANOVA)

Discussion

This study shows that CBL traits differ between small-polyped coral species. In addition, we show that O_2 concentration gradients within the CBL may occur in different profile shapes, which differ in prevalence among species. The formation of these profile types was largely dependent on flow, with overall purely diffusive profiles dominating across flow conditions and more complex profiles prevailing under

low flow. Some species may present structurally complex profiles even in moderate water flows. Finally, we show that boundary layers with different O_2 profile types also differed in CBL traits.

CBL traits differ between species

CBL traits differed among the small-polyped species studied, with differences strongest for CBL thickness. Such CBL variability among small-polyped corals could be associated with coral morphology (Chan et al. 2016), small-scale morphological complexity (e.g., surface roughness or fractal dimensions; Reichert et al. 2017), and species-specific

features and behavior, including the size, density, and activity of polyps (Shashar et al. 1993; Malul et al. 2020; Li et al. 2021) and surface cilia (Shapiro et al. 2014; Pacherres et al. 2020). While corallite size is similar among the investigated species (global range 0.5–1.5 mm; Pichon and Veron 1976), polyp density differs (*A. cytherea*, 12 polyps cm⁻²; Irikawa et al. 2011; *P. verrucosa*, 129 polyps cm⁻²; Sier and Olive 1994; *P. cylindrica*, 67 polyps cm⁻²; Anthony 1999). Lower polyp density possibly results in lower hydrodynamic drag forces on the coral surface and, together with the weak feeding and cleaning ciliary currents reported for acroporids (Lewis and Price 1976; Stafford-Smith 1993), may explain the thinner CBL of *A. cytherea* compared to the other two species (Shapiro et al. 2014).

Differences in CBL thickness could also be attributed to spatial heterogeneity of surface topography in relation to the location of the microsensors measurement. Although the similarly thick CBL of *P. verrucosa* and *P. cylindrica* in our study was within ranges reported for other pocilloporids and poritids under similar flow conditions (Jimenez et al. 2011; Chan et al. 2016), up to ten times thicker CBLs have been reported for *Stylophora pistillata* (Shashar et al. 1993). In our study, CBL was measured above the coenosarc, where it is generally thinner but also more stable than in other areas of the coral because polyp behavior is less likely to disrupt it. In addition, we performed all measurements on the upstream side of coral fragments, which has a thinner CBL than the downstream side (Edmunds 2005; Murthy et al. 2023). Although our measurements were thus performed in a location assumed to be hydrodynamically similar for the tested species, differences in microscale flow conditions at the coral surface may still have occurred and could account for some of the CBL variability observed. These surface flow differences, however, would likely be generated by the coral itself or due to species differences in microtopography. Finally, CBL thickness displayed similar patterns in light and darkness across species, demonstrating the overall stability of this trait with variable light conditions.

Species differences in surface O₂ concentration and flux were only present in dark conditions in our study. *Pocillopora verrucosa* showed the largest depletion of surface O₂ concentration and highest dark flux, which may be related to its higher respiration rates compared to *A. cytherea* and *P. cylindrica* (Vetter et al. unpublished data). Furthermore, these patterns could also be due to differences in cilia activity. Although cilia activity has been shown to have no effect on O₂ flux across the CBL in light, it may enhance fluxes in the dark (Pacherres et al. 2020). This also suggests that cilia may have different roles during photosynthesis and dark respiration, with the latter depending on cilia activity to increase supply of O₂ during the night. Instead, during light, cilia appear to be important in reducing the risk of oxidative stress without modulating O₂ flux by redistributing

O₂ in the CBL over the coral surface and maintaining low O₂ levels above areas with high chlorophyll concentration (Ahmerkamp et al. 2022; Pacherres et al. 2022).

As expected, water flow modulated CBL traits across species, with largely consistent effects. CBL thickness generally increased with reduced flow, as seen previously (e.g., Shashar et al. 1993; Kühl et al. 1995), while surface O₂ was more depleted under low flow than under moderate flow, suggesting a lower O₂ exchange with bulk seawater under the low flow. O₂ flux, however, was affected by flow conditions only during darkness in our study. Dark flux was reduced under low flow compared to moderate flow, which is in agreement with previous reports of decreased coral respiration with reduced flow (e.g., Patterson et al. 1991). During the night, coral internal and surface O₂ concentrations are undersaturated and may reach extreme depletion (Shashar et al. 1993; Kühl et al. 1995). This can limit coral respiration (Sebens et al. 2003), indicating that it may be limited by the diffusive supply of O₂ from bulk seawater (Kühl et al. 1995; Gardella and Edmunds 1999). Altogether, our results provide further evidence for the O₂ limitation that corals may experience at night, which may be exacerbated during periods of low flow.

CBL profile types across species and water flow conditions

The combination of surface topography, ciliary movement, metabolic rates, and environmental conditions leads to differences in the type and distribution of CBL profiles. Diffusive profiles were the predominant profile type in our study, which is in agreement with previous observations under moderate water flow (Shashar et al. 1993; Kühl et al. 1995). The formation of these profiles is due to viscous forces dominating near the coral surface and making flow laminar and molecular diffusion the dominant mechanism of mass transport (Jørgensen and Revsbech 1985; Nishihara and Ackerman 2007). Our S-shaped profiles corresponded to the profile shapes created by the activity of epidermal cilia, previously observed only under near-zero flows (Shapiro et al. 2014; Pacherres et al. 2020). Similarly to S-shaped profiles, the presence of complex profiles could also be due to ciliary activity since these could occur in profiles that go through the middle of ciliary vortices (Shapiro et al. 2014) or as a result of complex flow patterns caused by the coral microtopography. For instance, model simulations show that surface structures such as verrucae may modulate and slow down flow near the coral surface (Hossain and Staples 2020). Furthermore, scleractinian corals also generate horizontal surface currents (Bouderlique et al. 2022), which could influence profile structure.

Ciliary vortices have previously been observed in several species, including *Acropora* sp., *Montipora* sp., *Seriatopora*

hystrix, *S. pistillata*, and *Favia* sp. (Shapiro et al. 2014). Therefore, S-shaped and complex profiles are expected to occur in a range of species as observed herein. The influence of cilia activity on surface conditions has been observed to be greatest with flow velocities below 1 cm s^{-1} because faster flow tends to erase the vortices created by beating cilia and the resulting profile structure (Shapiro et al. 2014; Murthy et al. 2023). While this explains the prevalence of diffusive profiles in our study, S-shaped profiles were more abundant under both flow conditions here than expected based on previous conceptual models (Shapiro et al. 2014).

In this study, all profile types were observed in each species, except *A. cytherea*, which did not have complex profiles. However, the frequency of distinct O_2 CBL profiles differed between species. Profiles of *A. cytherea* were mostly diffusive, while *P. verrucosa* and *P. cylindrica* were characterized by a larger proportion of S-shaped and complex profiles. These differences in profile types may underlie differences in coral growth or photosynthesis. Both *A. cytherea* and *P. verrucosa* are fast-growing species and considered highly efficient at using environmental resources (Darling et al. 2012), which may be related to a prevalence of diffusive profiles with higher O_2 exchange across the coral surface. In contrast, branching *Porites* spp., such as *P. cylindrica*, have lower growth rates than *Acropora* spp. (Pratchett et al. 2015), which could be associated with a larger proportion of complex profiles, as observed herein.

Overall, the different frequency of profile types among the studied species may be indicative of their variable ability to alter the boundary layer, with potential downstream consequences on growth rates. Given the importance of mass transport to modulate coral colony physiology (Patterson et al. 1991), such differences may be key to understanding the response of coral species to changing environmental conditions (Schoepf et al. 2018).

Traits of CBL profile types

Boundary layers with different profile shapes differed in thickness and flux in our study, with complex profiles presenting the thickest CBL and lowest O_2 flux. Lower mass transfer associated with thick CBLs can limit photosynthesis, respiration, and calcification (Finelli et al. 2006; Colombo-Pallotta et al. 2010). Thick CBLs, however, also provide a better isolation from surrounding bulk seawater, which may be an advantage in the context of ocean acidification (Chan et al. 2016) and deoxygenation (Osinga et al. 2017; Hughes et al. 2020). Therefore, species with complex CBLs may be less vulnerable to ocean acidification and deoxygenation by reducing exposure to stressful conditions of bulk seawater (Noisette et al. 2022). In line with this, *P. cylindrica* has been shown to be less vulnerable to OA than *Acropora* spp. (Suggett et al. 2013; Martins et al. 2024a).

Our results of O_2 concentration at the coral surface among profile types, however, were unexpected. O_2 concentration varies along the coral surface (Pacherres et al. 2022), and particularly, within ciliary vortices. O_2 levels are generally reduced in the central and downward sections of vortices, which is associated with a mitigation strategy of high surface O_2 concentrations (Pacherres et al. 2020). In contrast, changes in surface O_2 concentration were similar between profile types in our study, which would rule out a direct link between surface O_2 levels and the formation of the different profile shapes. Alternatively, lower water flow conditions than those tested in our study may be necessary to observe differences in surface O_2 concentration among profile types.

Determining patterns and dynamics of the CBL is challenging due to spatial and temporal variability (Linsmayer et al. 2020; Pacherres et al. 2022). Spatial heterogeneity and coral circadian rhythms may present confounding factors when spot measurements are carried out throughout the day. Despite this, we detected significant patterns, which might be underestimated given the methodological approach. Further knowledge on CBL changes throughout a diel cycle will be essential for understanding the substantial CBL variability generally observed among species and environmental conditions across studies. Finally, future studies able of 3D mapping the CBL along the coral surface and better characterizing its spatial heterogeneity will help resolve the inter-specific variability of coral CBL traits.

Conclusions

Our study indicates that small-polyped reef-building corals may have different O_2 boundary layers. Using profile measurements performed in the laboratory, we show that (i) CBL traits differ between small-polyped species, regardless of flow conditions, which could be related to differences in surface cilia activity. In addition, we found that (ii) O_2 concentration gradients in the coral CBL may have different profile shapes (diffusive, S-shaped, and complex), which occur with varying frequency among coral species, depending on surface topography, ciliary movement, and environmental conditions, particularly water flow. We show that some species can present structurally complex profiles even in moderate water flows. These findings may be indicative of variable ability of coral species to alter their boundary layer, with potential downstream consequences on growth rates. However, the feedback loops between coral physiological activity and CBL traits could further contribute to species differences at both the colony and CBL scales. Finally, we found that (iii) boundary layers with different O_2 profile shapes may differ in CBL traits, which are modulated by water flow conditions. Such CBL variability could underlie

the range of sensitivities to climate change of reef-building corals and be key to understanding coral responses.

Overall, our findings show that CBL variability exists even among small-polyped coral species and highlight the benefit of accurately identifying the profile structure and traits of O₂ concentration gradients within the CBL to better understand the coral-seawater interface. The coral surface displays pronounced spatial and temporal variability, which may present confounding factors for studies based on spot measurements of the coral surface. Therefore, future 3D mappings of the CBL along the coral surface will help resolve the interspecific variability of coral CBL traits.

Acknowledgements This study was conducted as part of the ‘Ocean2100’ global change simulation project of the Colombian-German Center of Excellence in Marine Sciences (CEMarin), funded by the German Academic Exchange Service (DAAD, project number 57480468).

Author contributions CM, MW, and MZ designed the study. CM and PS set up the experiment and maintained animals. CM collected and analyzed the data and prepared the figures and tables. MW provided the microsensor measuring system. TW secured funding. CM drafted the manuscript with assistance from MZ. All authors contributed to editing and reviewing of the manuscript.

Funding Open Access funding enabled and organized by Projekt DEAL.

Data availability The raw data are available as part of a larger dataset of microsensor measurements at <https://doi.org/10.6084/m9.figshare.24534343>.

Declarations

Conflict of interest On behalf of all authors, the corresponding author states that there is no conflict of interest.

Open Access This article is licensed under a Creative Commons Attribution 4.0 International License, which permits use, sharing, adaptation, distribution and reproduction in any medium or format, as long as you give appropriate credit to the original author(s) and the source, provide a link to the Creative Commons licence, and indicate if changes were made. The images or other third party material in this article are included in the article’s Creative Commons licence, unless indicated otherwise in a credit line to the material. If material is not included in the article’s Creative Commons licence and your intended use is not permitted by statutory regulation or exceeds the permitted use, you will need to obtain permission directly from the copyright holder. To view a copy of this licence, visit <http://creativecommons.org/licenses/by/4.0/>.

References

Ahmerkamp S, Jalaluddin FM, Cui Y, Brumley DR, Pachterres CO, Berg JS, Stocker R, Kuypers MMM, Koren K, Behrendt L (2022) Simultaneous visualization of flow fields and oxygen concentrations to unravel transport and metabolic processes in biological systems. *Cell Reports Methods* 2:100216

- Anthony KRN (1999) Coral suspension feeding on fine particulate matter. *J Exp Mar Biol Ecol* 232:85–106
- Bates D, Mächler M, Bolker B, Walker S (2015) Fitting linear mixed-effects models using lme4. *J Stat Softw* 67:1–48
- Bouderlique T, Petersen J, Faure L, Abed-Navandi D, Bouchnita A, Mueller B, Nazarov M, Englmaier L, Tesarova M, Frade PR, Zikmund T, Koehne T, Kaiser J, Fried K, Wild C, Pantos O, Hellander A, Bythell J, Adameyko I (2022) Surface flow for colonial integration in reef-building corals. *Curr Biol* 32:2596–2609.e7
- Chan NCS, Wangpraseurt D, Köhl M, Connolly SR (2016) Flow and coral morphology control coral surface pH: implications for the effects of ocean acidification. *Front Mar Sci* 3:1–11
- Colombo-Pallotta MF, Rodríguez-Román A, Iglesias-Prieto R (2010) Calcification in bleached and unbleached *Montastraea faveolata*: evaluating the role of oxygen and glycerol. *Coral Reefs* 29:899–907
- Darling ES, Alvarez-Filip L, Oliver TA, McClanahan TR, Côté IM (2012) Evaluating life-history strategies of reef corals from species traits. *Ecol Lett* 15:1378–1386
- Edmunds PJ (2005) Effect of elevated temperature on aerobic respiration of coral recruits. *Mar Biol* 146:655–663
- Finelli CM, Helmuth BST, Pentcheff ND, Wethey DS (2006) Water flow influences oxygen transport and photosynthetic efficiency in corals. *Coral Reefs* 25:47–57
- Fox J, Weisberg S (2019) *An R companion to applied regression*. Sage, Thousand Oaks, CA
- Gardella DJ, Edmunds PJ (1999) The oxygen microenvironment adjacent to the tissue of the scleractinian *Dichocoenia stokesii* and its effects on symbiont metabolism. *Mar Biol* 135:289–295
- Hossain MM, Staples AE (2020) Effects of coral colony morphology on turbulent flow dynamics. *PLoS ONE* 15:1–25
- Hughes DJ, Alderdice R, Cooney C, Köhl M, Pernice M, Voolstra CR, Suggett DJ (2020) Coral reef survival under accelerating ocean deoxygenation. *Nat Clim Chang* 10:296–307
- Irikawa A, Casareto BE, Suzuki Y, Agostini S, Hidaka M, van Woessik R (2011) Growth anomalies on *Acropora cytherea* corals. *Mar Pollut Bull* 62:1702–1707
- Jimenez IM, Köhl M, Larkum AWD, Ralph PJ (2008) Heat budget and thermal microenvironment of shallow-water corals: Do massive corals get warmer than branching corals? *Limnol Oceanogr* 53:1548–1561
- Jimenez IM, Köhl M, Larkum AWD, Ralph PJ (2011) Effects of flow and colony morphology on the thermal boundary layer of corals. *J R Soc Interface* 8:1785–1795
- Jørgensen BB, Revsbech NP (1985) Diffusive boundary layers and the oxygen uptake of sediments and detritus. *Limnol Oceanogr* 30:111–122
- Köhl M, Cohen Y, Dalsgaard T, Jørgensen B, Revsbech N (1995) Microenvironment and photosynthesis of zooxanthellae in scleractinian corals studied with microsensors for O₂, pH and light. *Mar Ecol Prog Ser* 117:159–172
- Lenth RV (2021) Emmeans: estimated marginal means, aka least-squares means. R package version 1.6.2–1. <https://cran.r-project.org/package=emmeans>
- Lesser MP, Weis VM, Patterson MR, Jokiel PL (1994) Effects of morphology and water motion on carbon delivery and productivity in the reef coral, *Pocillopora damicornis* (Linnaeus): diffusion barriers, inorganic carbon limitation, and biochemical plasticity. *J Exp Mar Biol Ecol* 178:153–179
- Lewis JB, Price WS (1976) Patterns of ciliary currents in Atlantic reef corals and their functional significance. *J Zool* 178:77–89
- Li S, Roger LM, Kumar L, Lewinski NA, Klein-Seetharaman J, Gagnon A, Putnam HM, Yang J (2021) Digital image processing to detect subtle motion in stony coral. *Sci Rep* 11:7722

- Linsmayer LB, Deheyn DD, Tomanek L, Tresguerres M (2020) Dynamic regulation of coral energy metabolism throughout the diel cycle. *Sci Rep* 10:1–12
- Malul D, Holzman R, Shavit U (2020) Coral tentacle elasticity promotes an *out-of-phase* motion that improves mass transfer. *Proc R Soc B Biol Sci* 287:20200180
- Martins CPP, Simancas-Giraldo SM, Schubert P, Wall M, Wild C, Wilke T, Ziegler M (2024a) Short periods of decreased water flow may modulate long-term ocean acidification in reef-building corals. Preprint at bioRxiv
- Martins CPP, Ziegler M, Schubert P, Wilke T, Wall M (2024b) Effects of water flow and ocean acidification on oxygen and pH gradients in coral boundary layer. *Sci Rep* 14:12757
- Murthy S, Picioreanu C, Kühl M (2023) Modeling the radiative, thermal and chemical microenvironment of 3D scanned corals. *Front Mar Sci* 10:1–41
- Nishihara GN, Ackerman JD (2007) On the determination of mass transfer in a concentration boundary layer. *Limnol Oceanogr Methods* 5:88–96
- Noisette F, Pansch C, Wall M, Wahl M, Hurd CL (2022) Role of hydrodynamics in shaping chemical habitats and modulating the responses of coastal benthic systems to ocean global change. *Glob Chang Biol* 28:3812–3829
- Osinga R, Derksen-Hooijberg M, Wijgerde T, Verreth JAJ (2017) Interactive effects of oxygen, carbon dioxide and flow on photosynthesis and respiration in the scleractinian coral *Galaxea fascicularis*. *J Exp Biol* 220:2236–2242
- Pacherres CO, Ahmerkamp S, Schmidt-Grieb GM, Holtappels M, Richter C (2020) Ciliary vortex flows and oxygen dynamics in the coral boundary layer. *Sci Rep* 10:7541
- Pacherres CO, Ahmerkamp S, Koren K, Richter C, Holtappels M (2022) Ciliary flows in corals ventilate target areas of high photosynthetic oxygen production. *Curr Biol* 32:4150–4158.e3
- Patterson MR, Sebens KP, Olson RR (1991) In situ measurements of flow effects on primary production and dark respiration in reef corals. *Limnol Oceanogr* 36:936–948
- Pichon M, Veron JEN (1976) Scleractinia of Eastern Australia. Australian Govt. Pub. Service, Canberra
- Pratchett MS, Anderson KD, Hoogenboom MO, Widman E, Baird AH, Pandolfi JM, Edmunds PJ, Lough JM (2015) Spatial, temporal and taxonomic variation in coral growth—implications for the structure and function of coral reef ecosystems. *Oceanogr Mar Biol Annu Rev* 53:215–295
- Putnam HM, Barott KL, Ainsworth TD, Gates RD (2017) The vulnerability and resilience of reef-building corals. *Curr Biol* 27:R528–R540
- R Core Team (2021) R: a language and environment for statistical computing. R Foundation for Statistical Computing, Vienna, Austria
- Ramsing N, Gundersen J (2023) Seawater and gases: tabulated physical parameters of interest to people working with microsensors in marine systems. Unisense. <https://unisense.com/technical-information/#tables>
- Reichert J, Backes AR, Schubert P, Wilke T (2017) The power of 3D fractal dimensions for comparative shape and structural complexity analyses of irregularly shaped organisms. *Methods Ecol Evol* 8:1650–1658
- RStudio Team (2021) RStudio: integrated development environment for R. RStudio, PBC, Boston, MA
- Schoepf V, Cornwall CE, Pfeifer SM, Carrion SA, Alessi C, Comeau S, McCulloch MT (2018) Impacts of coral bleaching on pH and oxygen gradients across the coral concentration boundary layer: a microsensor study. *Coral Reefs* 37:1169–1180
- Sebens KP, Helmuth B, Carrington E, Agius B (2003) Effects of water flow on growth and energetics of the scleractinian coral *Agaricia tenuifolia* in Belize. *Coral Reefs* 22:35–47
- Shapiro OH, Fernandez VI, Garren M, Guasto JS, Debaillon-Vesque FP, Kramarsky-Winter E, Vardi A, Stocker R (2014) Vortical ciliary flows actively enhance mass transport in reef corals. *Proc Natl Acad Sci* 111:13391–13396
- Shashar N, Cohen Y, Loya Y (1993) Extreme diel fluctuations of oxygen in diffusive boundary layers surrounding stony corals. *Biol Bull* 185:455–461
- Shashar N, Kinane S, Jokiel PL, Patterson MR (1996) Hydromechanical boundary layers over a coral reef. *J Exp Mar Biol Ecol* 199:17–28
- Sier CJS, Olive PJW (1994) Reproduction and reproductive variability in the coral *Pocillopora verrucosa* from the Republic of Maldives. *Mar Biol* 118:713–722
- Stafford-Smith MG (1993) Sediment-rejection efficiency of 22 species of Australian scleractinian corals. *Mar Biol* 115:229–243
- Suggett DJ, Dong LF, Lawson T, Lawrenz E, Torres L, Smith DJ (2013) Light availability determines susceptibility of reef building corals to ocean acidification. *Coral Reefs* 32:327–337
- Thomas FIM, Atkinson MJ (1997) Ammonium uptake by coral reefs: effects of water velocity and surface roughness on mass transfer. *Limnol Oceanogr* 42:81–88
- Wickham H (2016) ggplot2: elegant graphics for data analysis. Springer-Verlag, New York

Publisher's Note Springer Nature remains neutral with regard to jurisdictional claims in published maps and institutional affiliations.